

See discussions, stats, and author profiles for this publication at: <https://www.researchgate.net/publication/286447966>

# A New Pulley Stress Analysis Method Based on Modified Transfer Matrix

Article in Bulk Solids Handling · November 1993

---

CITATIONS

10

READS

151

1 author:



Xiangjun Qiu

Metso Minerals

17 PUBLICATIONS 230 CITATIONS

SEE PROFILE

Some of the authors of this publication are also working on these related projects:



rolling resistance model [View project](#)



Conveyor Pulley Design and Analysis [View project](#)

# A New Pulley Stress Analysis Method Based on Modified Transfer Matrix

Xiangjun Qiu and Vinit Sethi, USA

## Summary

A new pulley stress analysis method is presented. It shall be referred to as the Modified Transfer Matrix (MTM) method. This method is based on a reformulation of transfer matrices for the pulley's cylindrical shell, end-disk plate with non-uniform thickness and shaft by using finite element concepts. It combines the strength of both classical stress analysis methods and finite element methods. It proves to be an efficient and effective approach in determining the stresses in a pulley. A pulley stress analysis software program named PSTRESS 3.0 has been developed based on this new method. At the end of the paper, a numerical example of the pulley stress analysis, using PSTRESS 3.0, is given. The result is satisfactorily compared with that obtained in a finite element model (ANSYS) solution with a very fine mesh.

## Nomenclature

$x$	Cartesian coordinate in horizontal direction	$I$	identity matrix
$y$	Cartesian coordinate in vertical direction	$K_{BM}$	TMB beam element stiffness matrix
$z$	Cartesian coordinate in pulley axial direction	$U_{BM}$	TMB beam element displacement vector
$r$	cylindrical coordinate in pulley radial direction	$F_{ext}^{BM}$	TMB beam element external force vector
$\phi$	cylindrical coordinate in pulley circumferential direction	$F_{int}^{BM}$	TMB beam element internal force vector
$P$	shear force acting on shaft cross section	$Q_r$	transverse shear force acting on the disk cross section perpendicular to radial direction
$M$	bending moment acting on shaft cross section	$Q_\phi$	transverse shear force acting on the disk cross section perpendicular to circumferential direction
$q$	distributed load acting on shaft axis	$M_r$	bending moment acting on the disk cross section perpendicular to disk radial direction
$w_s$	transverse displacement of shaft neutral axis	$M_\phi$	bending moment acting on the disk cross section perpendicular to disk circumferential direction
$\theta_s$	rotational angle of shaft cross section	$M_{r\phi}$	twisting moment acting on the disk cross sections perpendicular to disk radial direction and disk circumferential direction
$EI$	shaft bending stiffness	$g$	external transverse force acting on the neutral surface of the disk
$a$	shaft cross section area	$u$	pulley disk and shell displacements in pulley axial direction
$G$	shear modulus of shaft material	$v$	pulley disk and shell displacements in pulley circumferential direction
$\beta$	shaft state variable vector	$w$	pulley disk and shell displacements in pulley radial direction
$A$	matrix containing coefficients of governing ODEs for shaft bending deformation	$E$	YOUNG's modulus of disk or cylindrical shell of pulley
$B$	vector representing the non-homogeneous term of the governing ODEs for shaft bending deformation	$\mu$	Poisson's ratio of disk or cylindrical shell of pulley
$T$	transfer matrix for the governing ODEs for shaft bending deformation	$t$	thickness of disk or cylindrical shell of pulley
		$c$	coefficient to describe the geometry of disk variable thickness
		$p$	exponential number to describe the geometry of disk variable thickness
		$D$	cross section bending stiffness of disk or cylindrical shell
		$m$	FOURIER component number
		$u_m$	FOURIER component of $u$
		$v_m$	FOURIER component of $v$
		$w_m$	FOURIER component of $w$
		$g_m$	FOURIER component of $g$
		$Q_{rm}$	FOURIER component of $Q_r$
		$Q_{\phi m}$	FOURIER component of $Q_\phi$
		$M_{rm}$	FOURIER component of $M_r$
		$M_{\phi m}$	FOURIER component of $M_\phi$

Dr. Xiangjun Qiu, Director of Applied Mechanics, and Mr. Vinit Sethi, Research Engineer, Conveyor Dynamics Inc. (CDI), 1111 West Holly Street, Bellingham, WA 98225, USA. Tel.: +1 206 671 2200; Fax: +1 206 671 8450.

Details about the authors on page 896.

$M_{r\phi m}$	FOURIER component of $M_{r\phi}$	$f_z$	external load acting on the neutral surface of shell in pulley axial direction
$\theta_m$	rotational angle of disk or cylindrical shell of pulley	$f_\phi$	external load acting on the neutral surface of shell in pulley circumferential direction
$\gamma_m$	disk bending state variable vector of FOURIER component $m$	$f_r$	external load acting on the neutral surface of shell in pulley radial direction
$m_m$	disk circumferential harmonic resultant bending moment	$f_{zm}$	FOURIER component of $f_z$
$V_m$	disk circumferential harmonic resultant transverse shear force	$f_{\phi m}$	FOURIER component of $f_\phi$
$A_m$	matrix containing coefficients of governing ODEs for disk bending deformation of FOURIER component $m$	$f_{rm}$	FOURIER component of $f_r$
$B_m$	vector representing the non-homogeneous term of the governing ODEs for disk bending deformation of FOURIER component $m$	$N_{1m}$	FOURIER component of $N_1$
$U_m^{BD}$	TMB disk bending element displacement vector	$N_{2m}$	FOURIER component of $N_2$
$K_{BD m}$	TMB disk bending element stiffness matrix	$S_m$	FOURIER component of $S$
$F_{ext m}^{BD}$	TMB disk bending element external force vector	$M_{1m}$	FOURIER component of $M_1$
$F_{int m}^{BD}$	TMB disk bending element internal force vector	$M_{2m}$	FOURIER component of $M_2$
$N_r$	normal force acting on the disk cross section perpendicular to radial direction	$M_{12m}$	FOURIER component of $M_{12}$
$N_\phi$	normal force acting on the disk cross section perpendicular to circumferential direction	$V_{1m}$	FOURIER component of element boundary equivalent transverse shear force
$N_{r\phi}$	in-plane shear force acting on the disk cross sections perpendicular to disk radial direction and disk circumferential direction	$X_m$	cylindrical shell state variable vector of FOURIER component $m$
$N_{rm}$	FOURIER component of $N_r$	$J_m$	matrix containing coefficients of governing ODEs for cylindrical shell of FOURIER component $m$
$N_{\phi m}$	FOURIER component of $N_\phi$	$I_m$	vector representing the non-homogeneous term of the governing ODEs for cylindrical shell of FOURIER component $m$
$N_{r\phi m}$	FOURIER component of $N_{r\phi}$	$U_m^{CS}$	TMB cylindrical shell element displacement vector
$\eta_m$	disk plane-stress state variable vector of FOURIER component $m$	$K_{CS m}$	TMB cylindrical shell stiffness matrix
$C_m$	matrix containing coefficients of governing ODEs for disk in-plane deformation of FOURIER component $m$	$F_{ext m}^{CS}$	TMB cylindrical shell element external force vector
$U_m^{PN}$	TMB disk plane-stress element displacement vector	$F_{int m}^{CS}$	TMB cylindrical shell element internal force vector
$K_{PN m}$	TMB disk plane-stress element stiffness matrix	$\Psi_m$	state variable vector of FOURIER component $m$
$F_{ext m}^{PN}$	TMB disk plane-stress element external force vector	$s$	axial or radial coordinate
$F_{int m}^{PN}$	TMB disk plane-stress element internal force vector	$H_m$	matrix containing coefficients of governing ODEs of a pulley component
$U_m^{DK}$	TMB disk element displacement vector	$L_m$	vector representing the non-homogeneous term of the governing ODEs of a pulley component
$K_{DK m}$	TMB disk element stiffness matrix	$U_m$	generalized displacements of state variable vector of a pulley component
$F_{ext m}^{DK}$	TMB disk element external force vector	$F_m$	generalized forces of state variable vector of a pulley component
$F_{int m}^{DK}$	TMB disk element internal force vector	$T_m$	transfer matrix for the governing ODEs of a pulley component
$R$	cylindrical shell radius	$D_m$	TMB element displacement vector of a pulley component
$N_1$	normal force acting on the cylindrical shell cross section perpendicular to pulley axial direction	$K_m$	TMB element stiffness matrix of a pulley component
$N_2$	normal force acting on the cylindrical shell cross section perpendicular to pulley circumferential direction	$F_{int m}$	TMB element internal force vector of a pulley component
$S$	membrane shear force acting on the cylindrical shell cross sections perpendicular to pulley axial direction and circumferential direction	$F_{ext m}$	TMB element external force vector of a pulley component
$Q_1$	transverse shear force acting on the cylindrical shell cross section perpendicular to pulley axial direction		
$Q_2$	transverse shear force acting on the cylindrical shell cross section perpendicular to pulley circumferential direction		
$M_1$	bending moment acting on the cylindrical shell cross section perpendicular to pulley axial direction		
$M_2$	bending moment acting on the cylindrical shell cross section perpendicular to pulley circumferential direction		
$M_{12}$	twisting moment acting on the cylindrical shell cross sections perpendicular to pulley axial direction and circumferential direction		

## 1. Introduction

An engineered class belt conveyor pulley typically consists of a cylindrical shell, two end disks with variable thickness, a shaft, and two locking devices connecting end disks to the shaft as shown in Fig. 1. The pulley is usually subjected to severe bending due to very high belt tensions and locking assembly pressures. In the design of such a pulley, it is necessary to take into account the possibility of fatigue failure. Costly failures in large conveyor pulleys have led designers to seek detailed stress fatigue or endurance analysis. To date, two types of approaches for pulley stress analysis have been reported in the literature. One is the classical mechanics approach developed by LANGE

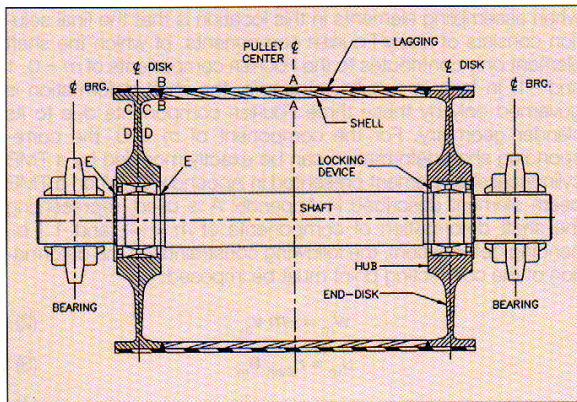


Fig. 1: Cross-section of pulley assembly

[1] and SCHMOLZI [2]. The other is the finite element method (FEM) employed by VODSTRCIL [3], DANIEL [4] and SETHI et al. [5]. Both types of approaches have advantages and disadvantages.

The classical mechanics approach developed by LANGE and SCHMOLZI is an approximate analytical approach, providing a closed-form solution for stresses in a pulley. The advantages of this method are that it is easy to program and takes a very short execution time to obtain a solution. The disadvantage is that the stress solution is not accurate at the locations near the connection region between the shell and end disks because of its poor approximation in treating the elastic coupling between these components. Specifically, the displacement of the end disk and shell are not coupled at their connection. This leads to significant errors in the stress and strain field about the connectors as will be shown.

The FEM has just the opposite advantages and disadvantages of the LANGE classical method. The major advantage of FEM is its ease of treating complex geometry and boundary conditions. The major disadvantage is its long execution time coupled with its need for an experienced user to generate a proper finite element mesh.

In this paper, a new method called the Modified Transfer Matrix (MTM) method is presented. This method circumvents the disadvantages of both the LANGE classical method and the conventional FEM. The MTM method proves to be a very effective and efficient approach in providing an accurate pulley assembly stress solution for any loading condition pulley.

Historically, the transfer matrix method was developed several decades ago [6] and was very popular in solving one dimensional static and dynamic problems before the advent of the FEM. Even today, this method is still useful in providing closed form solutions to certain elasticity problems with simple boundary conditions [7]. Although there is a limitation in handling complicated boundary conditions, such as the boundary conditions for a pulley, the solution obtained by using the transfer matrix method is exact. In this paper, it is shown that the limitation of the transfer matrix method can be overcome if the transfer matrix is reformulated by using finite element concepts. The reformulated transfer matrix is essentially a special finite element. The new method using these special finite elements, called transfer matrix based (TMB) finite elements, is capable of solving a class of structural elasticity problems (including the elasticity problem of a pulley), whose governing differential equations can be reduced to a set of ordinary differential equations (ODEs). Regardless of how few of these TMB finite elements are used in a model, the solution obtained by this MTM method is generally very accurate due to the nature of the transfer matrix method.

Based on the MTM method, a computer program for pulley stress analysis named PSTRESS 3.0 has been developed. This program can provide stress solutions and perform fatigue analysis for most pulleys, with the characteristic geometry shown in Fig. 1. The pulley can be subjected to any type of non-uniform surface pressure, shear loading, and prescribed locking pressure.

In section 2, the general ideas for deriving TMB elements for beam (i.e. shaft), end-disk plate with variable thickness, and cylindrical shell are presented. In section 3, the assembly of these elements to model a pulley in PSTRESS 3.0 is discussed. In section 4, an example of a belt conveyor pulley is numerically solved by PSTRESS 3.0 and the results are compared with those obtained using a finely meshed FEM (ANSYS) solution.

## 2. TMB Finite Elements for Beam, Disk Plate and Cylindrical Shell

Stresses and displacements in a pulley can be expressed in terms of FOURIER series with respect to the circumferential angle because of the pulley's axisymmetric geometry. Each FOURIER component of the solutions can be determined by solving a set of corresponding governing differential equations, which are uncoupled with the governing equations for other Fourier components. In Appendices A, B and C, it is shown that the governing equations for Fourier components for shaft, end-disk plate with non-uniform thickness, and cylindrical shell of a pulley can be reduced to a set of ODEs of the first order respectively. The general solutions to these ODEs can be expressed in terms of the transfer matrix. By following the procedure described in Appendix D, the general solutions can be reorganized in a finite element form as below

$$K_m D_m = F_{int\ m} + F_{ext\ m} \quad (1)$$

where  $K_m$  is the TMB element stiffness matrix,  $D_m$  is the element displacement vector,  $F_{int\ m}$  is the element internal force vector,  $F_{ext\ m}$  is the element external force vector, and the subscript "m" denotes the FOURIER component number. The detailed procedures of developing TMB elements for shaft, end-disk and cylindrical shell are given in Appendices A, B and C, respectively.

### Remarks:

As seen in the above discussion, the general solution to the governing differential equations for a pulley can be finally transformed into a finite-element form. This allows us to exploit many finite element analysis (FEA) capabilities to resolve pulley stresses using our MTM method. The most valuable FEA capability to be employed is the way of treating complicated boundary conditions. Therefore, using the MTM method, we can easily take into account the elastic coupling between the rim and the end-disk by following FEA assembly procedures, and implement the locking assembly pressure by using the FEA approach of treating mechanical interference between two bodies. Both of these problems cannot be easily or precisely handled by most classical methods.

## 3. Assembly of TMB Elements for a Pulley Model in PSTRESS 3.0

In PSTRESS 3.0, the above derived TMB beam, disk plate and cylindrical shell element stiffness matrices are brought together to form a global stiffness matrix for a pulley in essentially the same way as that in conventional FEM. However, care must be taken at two locations, where special element assembly methods are required.

The first location is the connection region between the shell and the disk shown in Fig. 2a, where the finite dimension of the joint has to be taken into account in the stiffness matrix. The conventional way of treating the whole region as a single node would cause significant error in stress solutions near this region. One of the reasonable ways of providing correct elastic stiffness to connect the rim and the disk is treating the whole region as a special element by applying a substructure method. In PSTRESS 3.0, such a special element shown in Fig. 2b is developed.

The second location is the connection point between the locking device and the shaft. One thing that must be kept in mind

when assembling elements in this location is that the final solution consists of many FOURIER components, of which the shaft element only contributes to the FOURIER components of  $m = 0, 1$  and  $-1$ . In fact, in a pulley structure, the shaft deformation is governed only by these three FOURIER components due to its slender geometry. For the component of  $m = 0$ , the corresponding shaft deformation can be exactly modeled by a TMB cylindrical shell element presented in Appendix C. When a TMB beam element described in Appendix A is used, representing the shaft deformation of components of  $m = -1$  and  $1$  (i.e., bending deformation), the following constraints on the deformation of the connecting point must be imposed:

$$w_m = -m v_m \quad (2)$$

$$u_m = r_{\text{shaft}} \theta_m \quad (3)$$

$$w_s = w_m \quad (4)$$

$$\theta_s = \theta_m \quad (5)$$

$w_s$  and  $\theta_s$  are the shaft deflection and rotational angle respectively at the connecting point, where the subscript  $s$  denotes shaft deformation. The general definitions of  $w_s$  and  $\theta_s$  are given in Appendix A.

$u_m, v_m, w_m$  and  $\theta_m$  are disk plate displacements and rotational angle at the connecting point, where the subscript  $m$  denotes the FOURIER component number:  $m = -1$  or  $1$ . The general definitions of  $u_m, v_m, w_m$  and  $\theta_m$  are given in Appendix B.  $r_{\text{shaft}}$  is the shaft radius at the connection point.

Such constraints are easy to implement in a finite element model by using FEA static condensation or penalty methods [10]. In PSTRESS 3.0, the static condensation method is employed. Finally, it must be pointed out that the TMB beam element stiffness matrix and corresponding nodal forces must be multiplied by a factor of 2 before they are assembled into global equations, due to the difference between actual forces and harmonic forces.

#### 4. Numerical Example

Consider the belt conveyor pulley shown in Fig. 1, which is supported on two bearings and subjected to a locking pressure of 115.71 mPa (16,778 psi) at the interface between the locking device and disk hub. The shell circumferential surface pressure and shear loading between circumferential angles of  $83^\circ$  and  $254^\circ$ , are developed from unequal belt tensions  $T_1 = 1,017.8$  kN (228,800 lb) and  $T_2 = 632.98$  kN (142,300 lb) shown in Fig. 3. The material properties and geometrical parameters of the pulley are given in Table 1. This pulley is analyzed by using PSTRESS 3.0, ANSYS 4.4 and CDI's derivation of LANGE's classical method, respectively. Because of symmetry, only one quarter of pulley cross section is modeled.

In the PSTRESS model, the rim is modeled with 2 TMB elements, the disk is modeled with 6 TMB elements, the shaft is modeled with 3 TMB elements, and 71 FOURIER components are used. The reason for using more TMB elements for the disk is the necessity of taking account of the non-uniform thickness of the disk. In the ANSYS FEA model, 5,000 axisymmetric structural solid elements (with non axis-symmetric loading) are employed in the 2-D cross-section. The use of the ANSYS FEM package to analyze a pulley is discussed in [5].

Figs. 4–7 show the PSTRESS numerical results compared with the ANSYS results. From these figures, it is seen that at location A of the rim and location D of the disk the agreement between the results of the MTM method and the results of the conventional FEM is good. At location B of the rim and location C of the disk the agreement is still good, but some inaccuracy is ob-

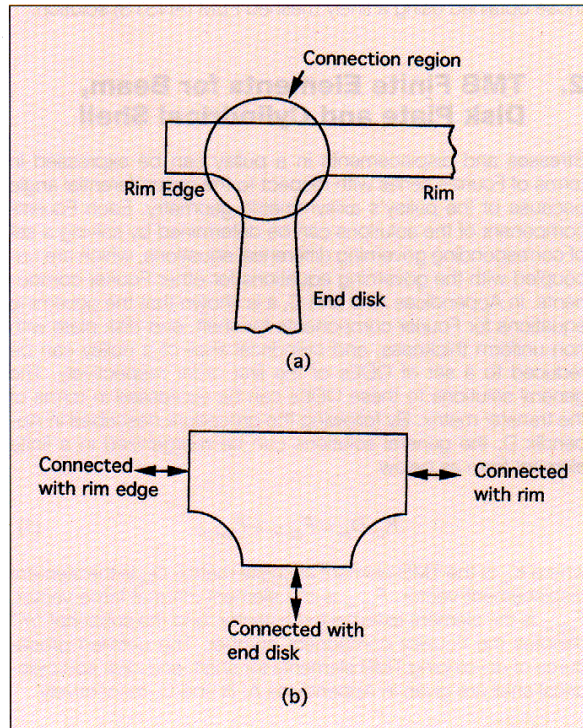
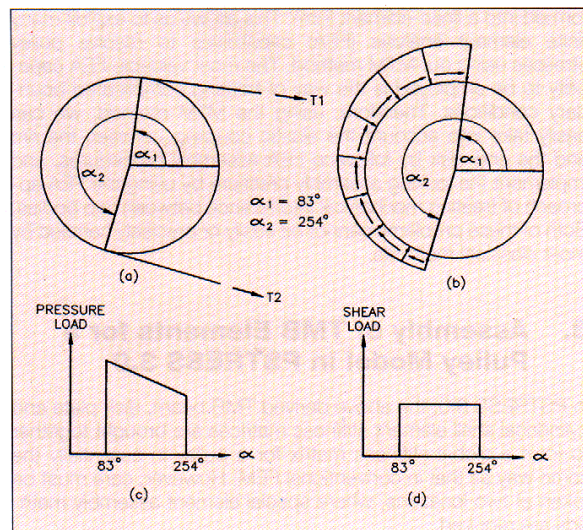


Fig. 2: Connecting element between rim and end-disk

Fig. 3: Load on pulley due to belt tension



Material Property		
YOUNG's modulus, MPSI		30
Poisson's ratio		0.3
Rim Geometry		
Rim length, inches		82
Rim outer diameter, inches		54
Rim thickness, inches		1.5
Belt width, inches		72
Disk Geometry		
Locking device width, inches		3.3
Hub outer diameter, inches		27.6
Hub inner diameter, inches		20.27
Hub width, inches		6.7
Fillet radius at hub, inches		3.67
Fillet radius at rim, inches		1.20
Disk thickness between hub and rim, inches		
Radius	Thickness	
1.	15.610	1.740
2.	16.268	1.487
3.	19.321	1.409
4.	22.400	1.217
5.	22.742	1.199
Shaft Geometry		
Diameter, inches		16.535
Shaft length, inches		121
Distance between bearing centres, inches		104
Distance between disk centres, inches		74.13

Table 1: Material properties and geometrical parameters

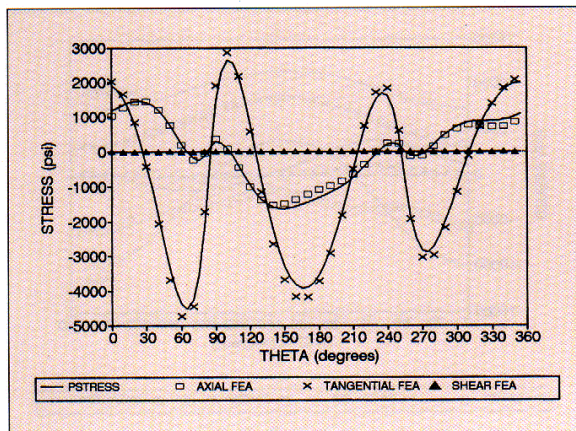


Fig. 4: Stresses at Location A (inside of rim) PSTRESS 3.0 Analysis

Fig. 6: Stresses at Location C (inside of disk) PSTRESS 3.0 Analysis

served. The reason may be that locations B and C are within the connection region between the rim and disk, where the 3-D stress state is more significant and cannot be fully taken into account in 2-D shell and plate theories. According to St. VENANTS principle and our experience, this 3-D stress state has only a very localized effect on pulley stress solution when the thicknesses of rim and disk are relatively small compared with the length and radius of the rim. It must be noted that the MTM method is much more efficient than the conventional FEM. PSTRESS 3.0 takes approximately 30 seconds to obtain a solution on an IBM PC 486, including the fatigue analysis. The FEM (ANSYS) solution takes 12-24 hours on an IBM RISC 6000 workstation.

Figs. 8-11 show the comparison of numerical results between LANGE's solution and the FEM solution. Except at location A, LANGE's solution does not agree with the FEM solution. The poor agreement is due to the errors in treating the elastic coupling between the rim and the end-disk in LANGE's method.

Figs. 12 and 13 show both the PSTRESS and ANSYS results at two corners of the interface between the locking device and the shaft (locations E-E of Fig. 1). At these two locations, 3-D stress state is much more significant than at locations B and C. In order to produce more accurate stress solutions at the two corners, we introduce stress concentration factors in zero and first order FOURIER component solutions by using our empirical formulae built in PSTRESS 3.0. As seen in Figs. 12 and 13, these corrected solutions agree well with ANSYS solutions.

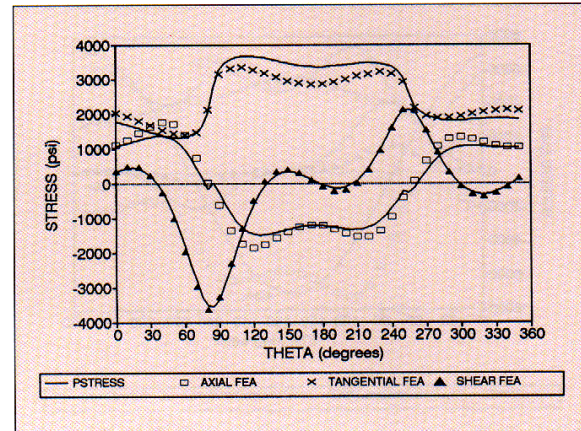
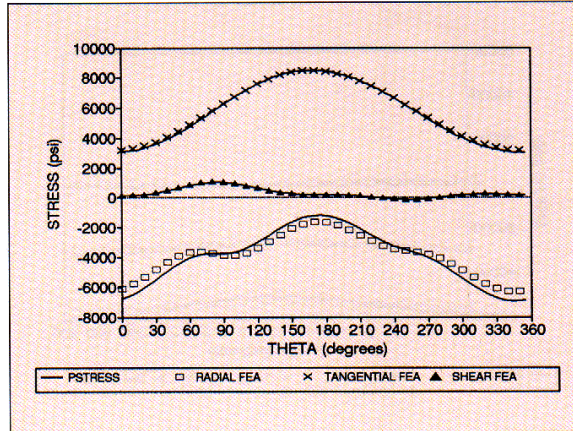
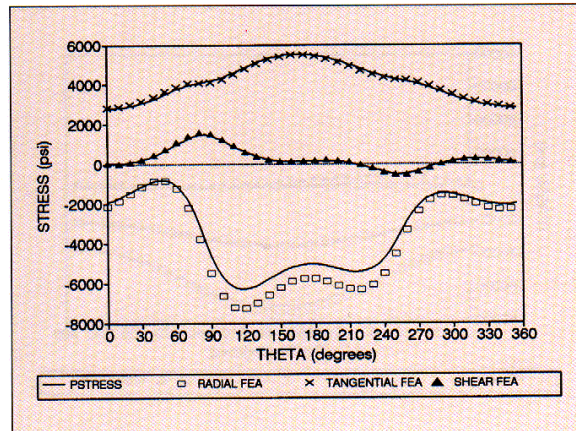


Fig. 5: Stresses at Location B (inside of rim) PSTRESS 3.0 Analysis

Fig. 7: Stresses at Location D (inside of disk) PSTRESS 3.0 Analysis



## 5. Conclusions

A new pulley stress analysis method which is based on reformulated transfer matrix has been developed. An accurate solution can be obtained by using this method. Three transfer-matrix-based elements for the shaft, disk plate and cylindrical shell have been developed. A numerical example has been given, which demonstrates the merits of this new method.

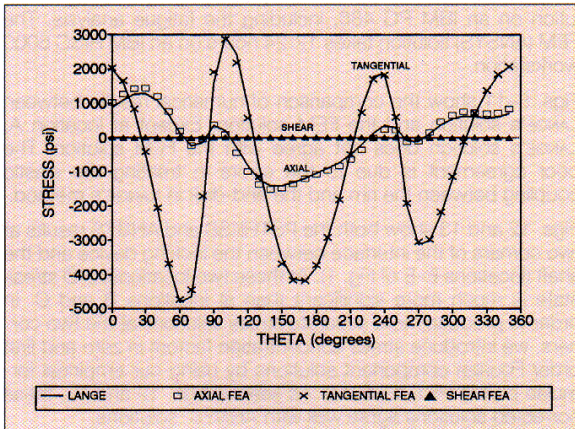


Fig. 8: Stresses at Location A (inside of rim) LANGE Analysis

## References

- [1] LANGE, H.: Investigations on Stress in Belt Conveyor Pulleys; Doctoral thesis, Technical University Hannover, 1963.
- [2] SCHMOLTZI, W.: The Design of Conveyor Belt Pulleys with Continuous Shafts; Doctoral thesis, Technical University, Hannover 1974.

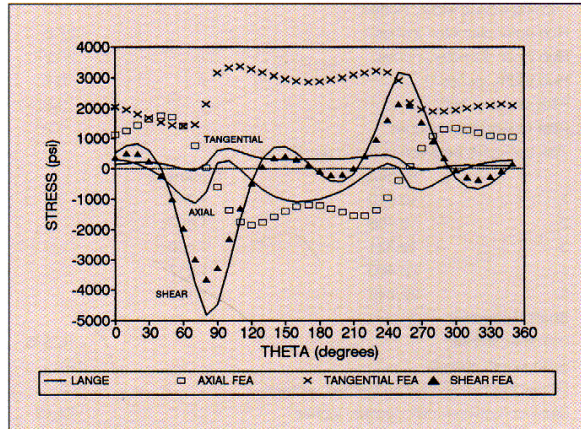


Fig. 9: Stresses at Location B (inside of rim) LANGE Analysis

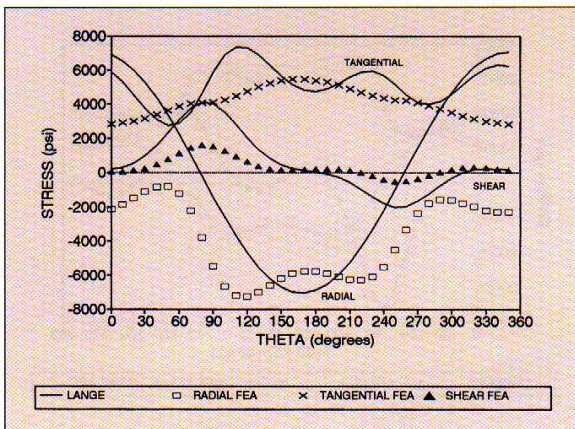


Fig. 10: Stresses at Location C (inside of disk) LANGE Analysis

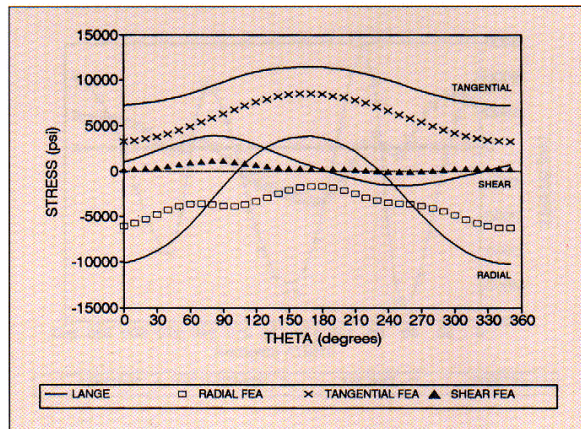


Fig. 11: Stresses at Location D (inside of disk) LANGE Analysis

Fig. 12: Stresses at Location E (inside of pulley) PSTRUSS 3.0 Analysis

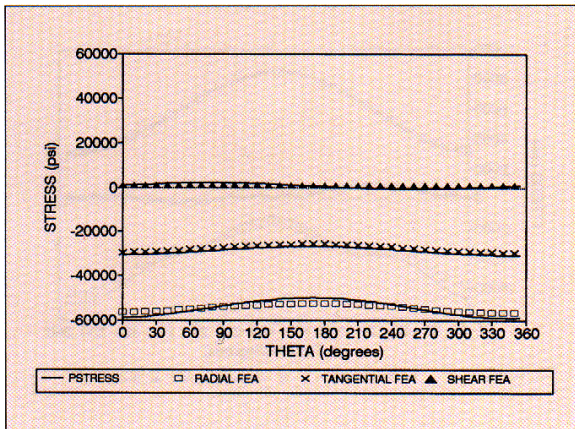
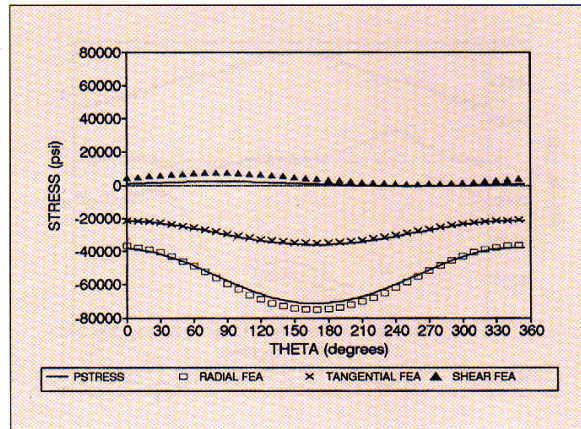


Fig. 13: Stresses at Location E outside of pulley) PSTRUSS 3.0 Analysis



- [3] VODSTRcil, R.: Analysis of Belt Conveyor Pulley Using Finite Element Method; Proc. 4th Int. Conf. in Australia on Finite Element Methods, University of Melbourne, Aug. 18-20, 1982.
- [4] DANIEL, W.J.T.: Development of a Conveyor Pulley Stress Analysis Package; Proc. Int. Conf. on Bulk Material Storage, Handling and Transportation, Newcastle, Aug. 22-24, 1983.
- [5] SETHI, V. and NORDELL, L.K.: Modern Pulley Design Techniques and Failure Analysis Methods; Proceedings of SME Annual Meeting & Exhibit, Reno Nevada, USA, Feb. 15-18, 1993.
- [6] PESTEL, E.C. and LECKIE, F.A.: Matrix Methods in Elastomechanics; New York McGraw-Hill Book Co., 1963.
- [7] YEH KAIYUAN: General Solution on Certain Problems of Elasticity with Non-Homogeneity and Variable Thickness, The Advances of Applied Mathematics and Mechanics, Vol. 1; China Academic Publishers, pp 240-273, 1987.
- [8] BOYCE, W.E. and DiPRIMA, R.C.: Elementary Differential Equations; Fifth Edition, John Wiley & Sons Inc., New York, 1992.
- [9] TIMOSHENKO, S. and WOINOWSKY-KRIEGER, S.: Theory of Plates and Shells; McGraw-Hill Book Co., Second Edition, 1959.
- [10] COOK, R.D., MALKUS, D.S. and PLESHA, M.E.: Concepts and Applications of Finite Element Analysis; Third Edition, John Wiley & Sons Inc., 1989.

## Appendix A

### TMB Finite Element for Beam

Fig. A1 shows forces that act on a differential beam. Loads  $P$ ,  $M$ , and  $q$  are shown in their positive sense.  $z$  is the axial coordinate. The equilibrium equations are

$$\frac{dP}{dz} = -q \quad (A1)$$

$$\frac{dM}{dz} = P \quad (A2)$$

By using TIMOSHENKO's beam theory, we have

$$\frac{dw_s}{dz} = -\theta_s + \frac{P}{kaG} \quad (A3)$$

$$\frac{d\theta_s}{dz} = \frac{M}{EI} \quad (A4)$$

where the subscript  $s$  denotes the shaft deformation,  $w_s$  is the shaft neutral axis displacement,  $-\theta_s$  is the slope due to bending,  $dw_s/dz$  is the slope of the center line of the beam,  $k$  is a shape factor equal to 0.75 for circular cross section,  $EI$  is the bending stiffness,  $a$  is the cross-section area, and  $G$  is the shear modulus.

Eqs. (A1)-(A4) can be written in a matrix form

$$\frac{d\beta}{dz} = A\beta + B \quad (A5)$$

where

$$\beta = (w_s, \theta_s, P, M)^T \quad (A6)$$

$$B = (0, 0, -q, 0)^T \quad (A7)$$

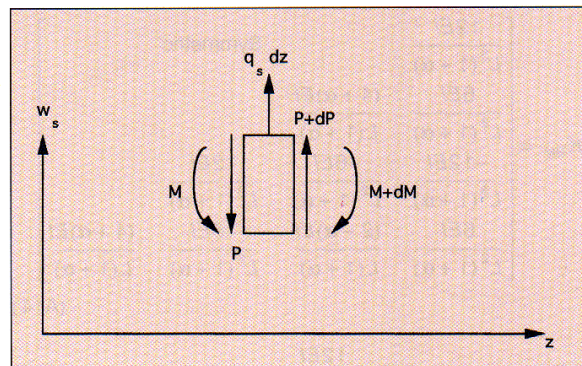


Fig. A1: Forces that act on a differential element of beam

$$\text{and } A = \begin{bmatrix} 0 & -1 & \frac{1}{kaG} & 0 \\ 0 & 0 & 0 & \frac{1}{EI} \\ 0 & 0 & 0 & 0 \\ 0 & 0 & 1 & 0 \end{bmatrix} \quad (A8)$$

where  $\beta$  is called state variable vector.

According to the ODE theory [8], the general solution to Eq. (A5) can be expressed as

$$\beta(z) = T(z)\beta(z_0) + T(z) \int_{z_0}^z T(s)^{-1} B(s) ds \quad (A9)$$

where  $z_0 \leq z \leq z_L$ ,  $z_0$  and  $z_L$  are the coordinates corresponding to two ends of the beam, and  $T(z)$  is the transfer matrix satisfying

$$\frac{dT}{dz} = AT \quad \text{and} \quad T(z_0) = I \quad (A10)$$

where  $I$  is the identity matrix. Following the general procedure described in [8], we can obtain the following closed-form transfer matrix

$$T(z) = \begin{bmatrix} 1 & z - z_0 & -\frac{z - z_0}{kaG} + \frac{(z - z_0)^3}{6EI} & \frac{(z - z_0)^2}{2EI} \\ 0 & 1 & \frac{(z - z_0)^2}{2EI} & \frac{z - z_0}{EI} \\ 0 & 0 & 1 & 0 \\ 0 & 0 & z - z_0 & 1 \end{bmatrix} \quad (A11)$$

where  $z_0 \leq z \leq z_L$ . Following the procedure described in Appendix D, we can obtain the following finite element equation, which is equivalent to Eq. (A9)

$$K_{BM} U_{BM} = F_{int}^{BM} + F_{ext}^{BM} \quad (A12)$$

where

$$U_{BM} = (w_s(z_L), \theta_s(z_L), w_s(z_0), \theta_s(z_0))^T \quad (A13)$$

$F_{ext}^{BM}$  is the beam element external force vector,  $F_{int}^{BM}$  is the beam element internal force vector, and  $K_{BM}$  is the beam element stiffness matrix, which can be expressed:

$$K_{BM} = \begin{bmatrix} \frac{12EI}{L^3(1+\alpha)} & & & \\ & \frac{6EI}{L^2(1+\alpha)} & \frac{(4+\alpha)EI}{L(1+\alpha)} & \\ & -\frac{12EI}{L^3(1+\alpha)} & \frac{-6EI}{L^2(1+\alpha)} & \frac{12EI}{L^3(1+\alpha)} \\ & \frac{6EI}{L^2(1+\alpha)} & \frac{(2-\alpha)EI}{L(1+\alpha)} & \frac{-6EI}{L^2(1+\alpha)} \\ & & \frac{(4+\alpha)EI}{L(1+\alpha)} & \end{bmatrix} \quad (A14)$$

$$\text{where } \alpha = \frac{12EI}{L^2kaG} \quad \text{and} \quad L = z_L - z_0 \quad (A15)$$

Remarks:

It is not surprising to note that the TMB finite element stiffness matrix for a beam derived as Eq. (A14) is identical to the beam stiffness matrix derived by using conventional finite element method because the polynomial-type trial function used in conventional FEM exactly represents the actual beam displacement. However, for other types of structures such as plate and shell, the TMB element stiffness matrices may not be the same as the conventional finite element stiffness matrices.

## Appendix B

### TMB Finite Element for Disk Plate with Variable Thickness

#### B.1 TMB Bending Element

Fig. B1 shows a differential element of plate subjected to bending loads.  $x$ ,  $y$  and  $z$  are Cartesian coordinates with  $z$  coinciding with pulley axial direction,  $x$  horizontal direction, and  $y$  vertical direction.  $r$  and  $\phi$  are disk cylindrical coordinates. Loads  $Q_r$ ,  $Q_\phi$ ,  $M_r$ ,  $M_\phi$  and  $M_{r\phi}$  are shown in their positive sense. The equilibrium equations are:

$$Q_r = \frac{\partial M_r}{\partial r} + \frac{M_r - M_\phi}{r} - \frac{1}{r} \frac{\partial M_{r\phi}}{\partial \phi} \quad (B1)$$

$$Q_\phi = \frac{\partial M_{r\phi}}{\partial r} + 2 \frac{M_{r\phi}}{r} - \frac{1}{r} \frac{\partial M_\phi}{\partial \phi} \quad (B2)$$

$$\frac{\partial Q_r}{\partial r} + \frac{Q_r}{r} - \frac{1}{r} \frac{\partial Q_\phi}{\partial \phi} = g(r, \phi) \quad (B3)$$

where  $g$  is the external transverse force acting on the neutral surface of the plate, and equations representing the force-deformation relationship are :

$$M_r = -D \left[ \frac{\partial^2 u}{\partial r^2} + \mu \left( \frac{1}{r} \frac{\partial u}{\partial r} + \frac{1}{r^2} \frac{\partial^2 u}{\partial \phi^2} \right) \right] \quad (B4)$$

$$M_\phi = -D \left[ \mu \frac{\partial^2 u}{\partial r^2} + \frac{1}{r} \frac{\partial u}{\partial r} + \frac{1}{r^2} \frac{\partial^2 u}{\partial \phi^2} \right] \quad (B5)$$

$$M_{r\phi} = D(1-\mu) \left[ \frac{1}{r} \frac{\partial^2 u}{\partial r \partial \phi} - \frac{1}{r^2} \frac{\partial u}{\partial \phi} \right] \quad (B6)$$

where  $u$  is the plate neutral surface transverse displacement (see Fig. B1),  $\mu$  is the Poisson's ratio,

$$D = \frac{Et^3}{12(1-\mu^2)} \quad (B7)$$

$E$  is the Young's modulus,  $t$  is the thickness of the plate, which is a function of  $r$ . Within the element, we assume

$$t = cr^p \quad (B8)$$

where  $c$  and  $p$  are constants. Also, we assume the following FOURIER series for the components of displacement and forces

$$u = \sum_{m=0}^{\infty} u_m \cos m\phi + \sum_{m=1}^{\infty} u_{-m} \sin m\phi \quad (B9)$$

$$g = \sum_{m=0}^{\infty} g_m \cos m\phi + \sum_{m=1}^{\infty} g_{-m} \sin m\phi \quad (B10)$$

$$Q_r = \sum_{m=0}^{\infty} Q_{rm} \cos m\phi + \sum_{m=1}^{\infty} Q_{r,-m} \sin m\phi \quad (B11)$$

$$Q_\phi = \sum_{m=1}^{\infty} Q_{\phi m} \sin m\phi + \sum_{m=0}^{\infty} Q_{\phi,-m} \cos m\phi \quad (B12)$$

$$M_r = \sum_{m=0}^{\infty} M_{rm} \cos m\phi + \sum_{m=1}^{\infty} M_{r,-m} \sin m\phi \quad (B13)$$

$$M_\phi = \sum_{m=0}^{\infty} M_{\phi m} \cos m\phi + \sum_{m=1}^{\infty} M_{\phi,-m} \sin m\phi \quad (B14)$$

$$M_{r\phi} = \sum_{m=1}^{\infty} M_{r\phi m} \sin m\phi + \sum_{m=0}^{\infty} M_{r\phi,-m} \cos m\phi \quad (B15)$$

where  $u_m$ ,  $p_m$ ,  $Q_m$ ,  $Q_{\phi m}$ ,  $M_{rm}$ ,  $M_{\phi m}$ ,  $M_{r\phi m}$  ( $m = 0, \pm 1, \pm 2, \dots$ ) are functions of  $r$  only. Substituting Eqs. (B9)-(B15) into Eqs. (B1)-(B6), we have the following ordinary differential equations

$$Q_{rm} = M_{rm}' + \frac{1}{r} (M_{rm} - M_{\phi m}) - \frac{m}{r} M_{r\phi m} \quad (B16)$$

$$Q_{\phi m} = M_{\phi m}' + \frac{2}{r} M_{r\phi m} + \frac{m}{r} M_{\phi m} \quad (B17)$$

$$Q_{rm}' + \frac{1}{r} Q_{rm} - \frac{m}{r} Q_{\phi m} = g_m \quad (B18)$$

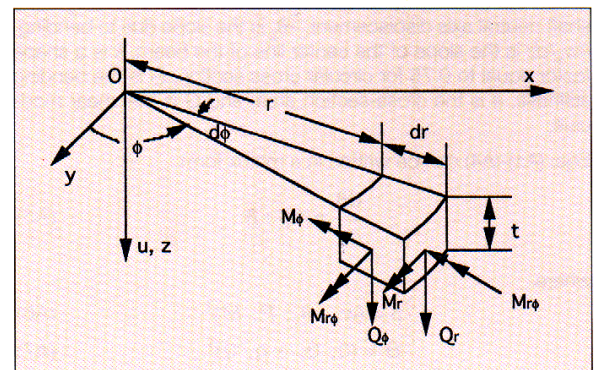
$$M_{rm} = -D \left[ u_m'' + \mu \left( \frac{1}{r} u_m' - \frac{m^2}{r^2} u_m \right) \right] \quad (B19)$$

$$M_{\phi m} = -D \left[ \mu u_m'' + \frac{1}{r} u_m' - \frac{m^2}{r^2} u_m \right] \quad (B20)$$

$$M_{r\phi m} = D(1-\mu) \left[ -\frac{m}{r} u_m' + \frac{m}{r^2} u_m \right] \quad (B21)$$

where  $m = 0, \pm 1, \pm 2, \dots$ , and the prime represents derivative with respect to  $r$ . Introducing the following state variables

Fig. B1: Bending forces that act on a differential element of plate



$$\gamma_m = (u_m, \theta_m, V_m, m_{rm})^T \quad (B22)$$

where

$$\theta_m = u_m \quad (B23)$$

$$m_{rm} = -2\pi M_{rm} \quad (B24)$$

$$V_m = 2\pi \left( Q_{rm} - \frac{m}{r} M_{r\phi m} \right) \quad (B25)$$

Eliminating five variables,  $M_{rm}$ ,  $M_{\theta m}$ ,  $M_{r\theta m}$ ,  $Q_{rm}$ , and  $Q_{\theta m}$  among Eqs. (B16)-(B21) and (B23)-(B25), we can obtain the following matrix-form equation

$$\frac{d\gamma_m}{dr} = A_m \gamma_m + B_m \quad (m = 0, \pm 1, \pm 2, \dots) \quad (B26)$$

where  $A_m =$

$$\begin{bmatrix} 0 & 1 & 0 & 0 \\ \frac{\mu m^2}{r^2} & -\frac{\mu}{r} & 0 & \frac{1}{2\pi D r} \\ \frac{2\pi D m^2 (2 - 2\mu + m^2 - m^2 \mu^2)}{r^3} & \frac{-2\pi D m^2 (3 - 2\mu - \mu^2)}{r^2} & -\frac{1}{r} & -\frac{\mu n^2}{r^2} \\ \frac{2\pi D m^2 (-3 + 2\mu + \mu^2)}{r^2} & \frac{2\pi D (1 - \mu^2 + 2m^2 - 2\mu m^2)}{r} & -1 & -\frac{(1-\mu)}{r} \end{bmatrix} \quad (B27)$$

$$B_m = (0, 0, 2\pi g_m, 0)^T \quad (B28)$$

Therefore, following the procedure described in Appendix D, we can obtain the following finite element equation for a circular plate ring ( $r_0 \leq r \leq r_L$ ) with variable thickness and subjected to harmonic bending load

$$K_{BD,m} U_m^{BD} = F_{int,m}^{BD} + F_{ext,m}^{BD} \quad (B29)$$

where

$$U_m^{BD} = (u_{Lm}, \phi_{Lm}, u_{0m}, \theta_{0m})^T \quad (B30)$$

$K_{BD,m}$  is the plate element bending stiffness matrix,  $F_{ext,m}^{BD}$  is the element external force vector,  $F_{int,m}^{BD}$  is the element internal force vector, the subscript  $L$  and  $0$  denote locations at  $r = r_L$  and  $r_0$ , respectively, and  $m$  denotes the FOURIER component number. Due to the complexity in deriving the transfer matrix for Eq. (B26), it is much more difficult to obtain a closed-form expression for  $K_{BD,m}$  of Eq. (B29) than for  $K_{BM}$  of Eq. (A12). Instead, we can very accurately calculate  $K_{BD,m}$  by using our computer program of PSTRESS 3.0 mentioned in Remark ii of Appendix D.

## B.2 TBM Plane Stress Element

Fig. B2 shows a differential element of plate subjected to in-plane loading. Loads  $N_r$ ,  $N_\phi$ , and  $N_{r\phi}$  are shown in their positive sense. The definitions of  $x$ ,  $y$ ,  $z$ ,  $r$  and  $\phi$  are the same as in section B.1. The equilibrium equations are

$$\frac{\partial N_r}{\partial r} + \frac{N_r - N_\phi}{r} + \frac{1}{r} \frac{\partial N_{r\phi}}{\partial \phi} = 0 \quad (B31)$$

$$\frac{\partial N_{r\phi}}{\partial r} + 2 \frac{N_{r\phi}}{r} + \frac{1}{r} \frac{\partial N_\phi}{\partial \phi} = 0 \quad (B32)$$

The equations for force-deformation relationship are

$$N_r = \frac{Et}{(1-\mu^2)} \left( \frac{\partial w}{\partial r} + \mu \frac{1}{r} \frac{\partial v}{\partial \phi} + \mu \frac{w}{r} \right) \quad (B33)$$

$$N_\phi = \frac{Et}{(1-\mu^2)} \left( \mu \frac{\partial w}{\partial r} + \frac{1}{r} \frac{\partial v}{\partial \phi} + \frac{w}{r} \right) \quad (B34)$$

$$N_{r\phi} = \frac{Et}{2(1+\mu)} \left( \frac{\partial v}{\partial r} + \frac{1}{r} \frac{\partial w}{\partial \phi} - \frac{v}{r} \right) \quad (B35)$$

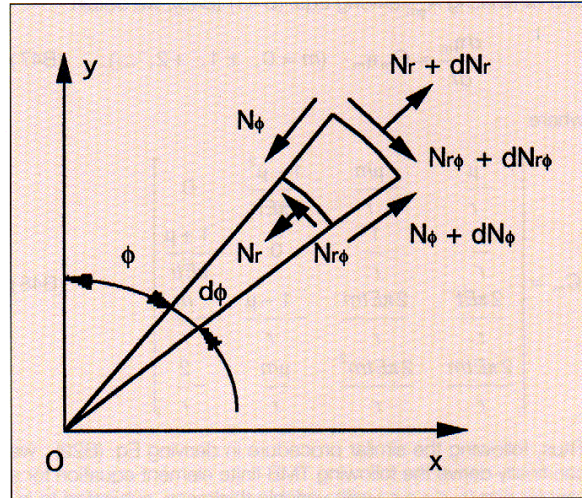


Fig. B2: In-plane forces that act on a differential element of plate

where the definitions of  $\mu$ ,  $E$  and  $t$  are the same as in section B.1, and  $v$  and  $w$  are the displacements of the neutral surface in circumferential and radial directions, respectively.

We assume the following FOURIER series for the components of displacements and forces

$$v = \sum_{m=1}^{\infty} v_m \sin m\phi + \sum_{m=0}^{\infty} v_{-m} \cos m\phi \quad (B36)$$

$$w = \sum_{m=0}^{\infty} w_m \cos m\phi + \sum_{m=1}^{\infty} w_{-m} \sin m\phi \quad (B37)$$

$$N_r = \sum_{m=0}^{\infty} N_{rm} \cos m\phi + \sum_{m=1}^{\infty} N_{r,-m} \sin m\phi \quad (B38)$$

$$N_\phi = \sum_{m=0}^{\infty} N_{\phi m} \cos m\phi + \sum_{m=1}^{\infty} N_{\phi,-m} \sin m\phi \quad (B39)$$

$$N_{r\phi} = \sum_{m=1}^{\infty} N_{r\phi m} \sin m\phi + \sum_{m=0}^{\infty} N_{r\phi m} \cos m\phi \quad (B40)$$

where  $v_m$ ,  $w_m$ ,  $N_{rm}$ ,  $N_{\phi m}$ , and  $N_{r\phi m}$  ( $m = 0, \pm 1, \pm 2, \dots$ ) are functions of  $r$  only. Substituting Eqs. (B36)-(B40) into Eqs. (B31)-(B35), we have the following ordinary differential equations

$$N_{rm}' + \frac{1}{r} (N_{rm} - N_{\phi m}) + \frac{m}{r} N_{r\phi m} = 0 \quad (B41)$$

$$N_{r\phi m}' + \frac{2}{r} N_{r\phi m} - \frac{m}{r} N_{\phi m} = 0 \quad (B42)$$

$$N_{rm} = \frac{Et}{(1-\mu^2)} \left[ w_m' + \mu \left( \frac{m}{r} v_m + \frac{1}{r} w_m \right) \right] \quad (B43)$$

$$N_{\phi m} = \frac{Et}{(1-\mu^2)} \left[ \mu w_m' + \frac{m}{r} v_m + \frac{1}{r} w_m \right] \quad (B44)$$

$$N_{r\phi m} = \frac{Et}{2(1+\mu)} \left[ v_m' - \frac{m}{r} w_m - \frac{1}{r} v_m \right] \quad (B45)$$

where  $m = 0, \pm 1, \pm 2, \pm 3, \dots$ . Introducing the following state variables

$$\eta_m = (w_m, v_m, 2\pi r N_{rm}, 2\pi r N_{r\phi m})^T \quad (B46)$$

and eliminating  $N_{\phi m}$  among Eqs. (B41)-(B45), we obtain

$$\frac{d\eta_m}{dr} = C_m \eta_m \quad (m = 0, \pm 1, +2, \dots) \quad (\text{B47})$$

where

$$C_m = \begin{bmatrix} -\frac{\mu}{r} & -\frac{\mu m}{r} & \frac{1-\mu^2}{2\pi E r} & 0 \\ m & \frac{1}{r} & 0 & \frac{1+\mu}{\pi E r} \\ \frac{2\pi E t}{r} & \frac{2\pi E t m}{r} & \frac{1-\mu}{r} & \frac{m}{r} \\ \frac{2\pi E t m}{r} & \frac{2\pi E t m^2}{r} & \frac{\mu m}{r} & \frac{2}{r} \end{bmatrix} \quad (\text{B48})$$

Thus, following the similar procedure in deriving Eq. (B29), we can finally derive the following TMB finite element equation for a circular ring ( $r_0 \leq r \leq r_L$ ) with variable thickness, subjected to in-plane harmonic loading

$$K_{PN m} U_m^{PN} = F_{int m}^{PN} + F_{ext m}^{PN} \quad (\text{B49})$$

where

$$U_m^{PN} = (w_{Lm}, v_{Lm}, w_{0m}, v_{0m})^T \quad (\text{B50})$$

$K_{PN m}$  is the element plane-stress stiffness matrix,  $F_{ext m}^{PN}$  is the element external force vector,  $F_{int m}^{PN}$  is the element internal force vector, and the subscript  $L$  and  $0$  denote locations at  $r = r_L$  and  $r_0$ , respectively, and  $m$  denotes the FOURIER component number.

Combining Eq. (B29) and Eq. (B49), we can form a TMB shell element for disk plate, which is subjected to both bending and in-plane loading

$$K_{DK m} U_m^{DK} = F_{int m}^{DK} + F_{ext m}^{DK} \quad (\text{B51})$$

where  $K_{DK m}$  is the disk element stiffness matrix,  $U_m^{DK}$  is the element displacement vector,  $F_{ext m}^{DK}$  is the element external force vector, and  $F_{int m}^{DK}$  is the element internal force vector. They can be calculated by the following formulae

$$U_m^{DK} = (u_{Lm}, v_{Lm}, w_{Lm}, \theta_{Lm}, u_{0m}, v_{0m}, w_{0m}, \theta_{0m})^T \quad (\text{B52})$$

$$K_{DK m} = S_1^T K_{BD m} S_1 + S_2^T K_{PN m} S_2 \quad (\text{B53})$$

$$F_{int m}^{DK} = S_1^T F_{int m}^{BD} + S_2^T F_{int m}^{PN} \quad (\text{B54})$$

$$F_{ext m}^{DK} = S_1^T F_{ext m}^{BD} + S_2^T F_{ext m}^{PN} \quad (\text{B55})$$

$$S_1 = \begin{bmatrix} 1 & 0 & 0 & 0 & 0 & 0 & 0 & 0 \\ 0 & 0 & 0 & 1 & 0 & 0 & 0 & 0 \\ 0 & 0 & 0 & 0 & 1 & 0 & 0 & 0 \\ 0 & 0 & 0 & 0 & 0 & 0 & 0 & 1 \end{bmatrix} \quad (\text{B56})$$

Remarks:

- iv. Any other state variables than those defined in Eq. (B22) and Eq. (B46) cannot be employed because they may lead to incorrect element stiffness matrices and force vectors due to the violation of MAXWELL's reciprocal theorem.
- v. Stiffness matrices obtained from transfer matrices must be symmetric. Any mistakes in choosing state variables, in deriving equations, and/or in numerical programming may lead to asymmetric stiffness matrices.

vi. If the stress calculation is desired, we can follow the following steps

- a. calculate values of state variables at element nodes,
- b. use transfer matrix and Eq. (D3) to calculate values of state variables at any interior location of the element, where stress values are desired,
- c. calculate first derivatives of state variables at desired locations by using Eq. (B26) and Eq. (B47),
- d. calculate  $M_{rm}$ ,  $M_{\phi rm}$ ,  $M_{r\phi rm}$ ,  $N_{rm}$ ,  $N_{\phi rm}$  and  $N_{r\phi rm}$  by using Eqs. (B19)-(B21) and Eqs. (B43)-(B45), and
- e. calculate FOURIER components of stresses by using calculated forces in step d.

## Appendix C

### TMB Finite Element for Cylindrical Shell

Fig. C1 shows forces acting on a differential element of a cylindrical shell with constant thickness  $t$  and radius  $R$ ,  $z$  and  $\phi$  are cylindrical coordinates. Loads  $N_1$ ,  $N_2$ ,  $S$ ,  $Q_1$ ,  $Q_2$ ,  $M_1$ ,  $M_2$  and  $M_{12}$  are shown in their positive sense. The equilibrium equations, according to [9], are

$$\frac{\partial N_1}{\partial z} + \frac{\partial S}{R \partial \phi} + f_z = 0 \quad (\text{C1})$$

$$\frac{\partial N_2}{R \partial \phi} + \frac{\partial S}{\partial z} + f_\phi = 0 \quad (\text{C2})$$

$$-\frac{N_2}{R} + \frac{\partial Q_1}{\partial z} + \frac{\partial Q_2}{R \partial \phi} + f_r = 0 \quad (\text{C3})$$

$$Q_2 = \frac{\partial M_{12}}{\partial z} + \frac{\partial M_2}{R \partial \phi} \quad (\text{C4})$$

$$Q_1 = \frac{\partial M_1}{\partial z} + \frac{\partial M_{12}}{R \partial \phi} \quad (\text{C5})$$

where  $f_z$ ,  $f_\phi$ , and  $f_r$  are external loads acting on the neutral surface of the shell in axial, circumferential and radial directions respectively, and the equations for force-displacement relationship, according to [9], are

$$N_1 = \frac{Et}{(1-\mu^2)} \left( \frac{\partial u}{\partial z} + \mu \frac{\partial v}{R \partial \phi} + \mu \frac{w}{R} \right) \quad (\text{C6})$$

$$N_2 = \frac{Et}{(1-\mu^2)} \left( \mu \frac{\partial u}{\partial z} + \frac{\partial v}{R \partial \phi} + \frac{w}{R} \right) \quad (\text{C7})$$

$$S = \frac{Et}{2(1+\mu)} \left( \frac{\partial u}{R \partial \phi} + \frac{\partial v}{\partial z} \right) \quad (\text{C8})$$

$$M_1 = -D \left( \frac{\partial^2 w}{\partial z^2} + \mu \frac{\partial^2 u}{R^2 \partial \phi^2} \right) \quad (\text{C9})$$

$$M_2 = -D \left( \mu \frac{\partial^2 w}{\partial z^2} + \frac{\partial^2 u}{R^2 \partial \phi^2} \right) \quad (\text{C10})$$

$$M_{12} = -(1-\mu)D \frac{\partial^2 w}{R \partial z \partial \phi} \quad (\text{C11})$$

where  $u$ ,  $v$  and  $w$  are shell neutral surface displacements in axial, circumferential and radial directions, respectively,

$$D = \frac{Et^3}{12(1-\mu)}$$

the definitions of  $E$  and  $\mu$  are the same as in section B, and  $t$  is the constant shell thickness. We assume the following FOURIER components of displacements and forces

$$f_z = \sum_{m=0}^{\infty} f_{zm} \cos m\phi + \sum_{m=1}^{\infty} f_{z,-m} \sin m\phi \quad (C12)$$

$$f_{\phi} = \sum_{m=1}^{\infty} f_{\phi m} \sin m\phi + \sum_{m=0}^{\infty} f_{\phi,-m} \cos m\phi \quad (C13)$$

$$f_r = \sum_{m=0}^{\infty} f_{rm} \cos m\phi + \sum_{m=1}^{\infty} f_{r,-m} \sin m\phi \quad (C14)$$

$$u = \sum_{m=0}^{\infty} u_m \cos m\phi + \sum_{m=1}^{\infty} u_{-m} \sin m\phi \quad (C15)$$

$$v = \sum_{m=1}^{\infty} v_m \sin m\phi + \sum_{m=0}^{\infty} v_{-m} \cos m\phi \quad (C16)$$

$$w = \sum_{m=0}^{\infty} w_m \cos m\phi + \sum_{m=1}^{\infty} w_{-m} \sin m\phi \quad (C17)$$

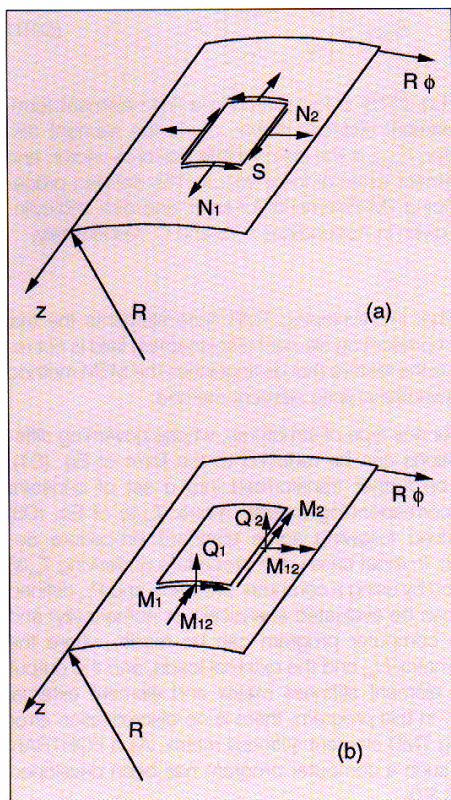
$$N_1 = \sum_{m=0}^{\infty} N_{1m} \cos m\phi + \sum_{m=1}^{\infty} N_{1,-m} \sin m\phi \quad (C18)$$

$$N_2 = \sum_{m=0}^{\infty} N_{2m} \cos m\phi + \sum_{m=1}^{\infty} N_{2,-m} \sin m\phi \quad (C19)$$

$$S = \sum_{m=1}^{\infty} S_m \sin m\phi + \sum_{m=0}^{\infty} S_{-m} \cos m\phi \quad (C20)$$

$$M_1 = \sum_{m=0}^{\infty} M_{1m} \cos m\phi + \sum_{m=1}^{\infty} M_{1,-m} \sin m\phi \quad (C21)$$

Fig. C1: Forces that act on a differential element of cylindrical



$$M_2 = \sum_{m=0}^{\infty} M_{2m} \cos m\phi + \sum_{m=1}^{\infty} M_{2,-m} \sin m\phi \quad (C22)$$

$$M_{12} = \sum_{m=1}^{\infty} M_{12m} \sin m\phi + \sum_{m=0}^{\infty} M_{12,-m} \cos m\phi \quad (C23)$$

$$Q_1 = \sum_{m=0}^{\infty} Q_{1m} \cos m\phi + \sum_{m=1}^{\infty} Q_{1,-m} \sin m\phi \quad (C24)$$

$$Q_2 = \sum_{m=1}^{\infty} Q_{2m} \sin m\phi + \sum_{m=0}^{\infty} Q_{2,-m} \cos m\phi \quad (C25)$$

where all FOURIER coefficients are functions of  $z$  only. Substituting Eqs. (C12)-(C25) into Eqs. (C1)-(C11), introducing the following state variables

$$\xi_m = (u_m, v_m, w_m, \theta_m, 2\pi RN_{1m}, 2\pi RS_m, 2\pi RV_{1m}, 2\pi RM_{1m})^T \quad (C26)$$

$$\text{where } \theta_m = -w_m \quad (C27)$$

$$\text{and } V_{1m} = Q_{1m} + \frac{m}{R} M_{12m} \quad (C28)$$

and eliminating five variables,  $N_{2m}$ ,  $M_{2m}$ ,  $M_{12m}$ ,  $Q_{1m}$ , and  $Q_{2m}$ , we can finally obtain the following matrix-form equation after a long tedious procedure of mathematical derivation

$$\frac{d\xi_m}{dz} = J_m \xi_m + l_m \quad (m = 0, \pm 1, \pm 2, \dots) \quad (C29)$$

where

$$J_m = \begin{bmatrix} 0 & -\frac{\mu m}{R} & -\frac{\mu}{R} & 0 & \frac{1-\mu^2}{2\pi EtR} & 0 & 0 & 0 \\ \frac{m}{R} & 0 & 0 & 0 & 0 & \frac{1+\mu}{\pi EtR} & 0 & 0 \\ 0 & 0 & 0 & -1 & 0 & 0 & 0 & 0 \\ 0 & 0 & -\frac{\mu m^2}{R^2} & 0 & 0 & 0 & 0 & \frac{6(1-\mu^2)}{\pi Et^3 R} \\ 0 & 0 & 0 & 0 & 0 & -\frac{m}{R} & 0 & 0 \\ 0 & \frac{2\pi Et m^2}{R} & \frac{2\pi Et m}{R} & 0 & \frac{\mu m}{R} & 0 & 0 & 0 \\ 0 & \frac{2\pi Et m}{R} & \frac{2\pi Et}{R} \left(1 + \frac{t^2 m^4}{12 R^2}\right) & 0 & \frac{\mu}{R} & 0 & 0 & \frac{\mu m^2}{R^2} \\ 0 & 0 & 0 & \frac{\pi Et^3 m^2}{3(1+\mu)R} & 0 & 0 & 1 & 0 \end{bmatrix} \quad (C30)$$

and

$$l_m = (0, 0, 0, 0, -2\pi R f_{zm}, -2\pi R f_{\phi m}, -2\pi R f_{rm}, 0)^T \quad (C31)$$

Therefore, according to the conclusions of Appendix D, the transfer matrix for Eq. (C29) can be obtained by the computer program developed in PSTRESS 3.0. Based on the transfer matrix, the TMB finite element for cylindrical shell with  $z_0 \leq z \leq z_L$  can be derived by following the procedure described in Appendix D, and the result can be expressed by

$$K_{CS,m} U_m^{CS} = F_{int,m}^{CS} + F_{ext,m}^{CS} \quad (C32)$$

where

$$U_m^{CS} = (u_{Lm}, v_{Lm}, w_{Lm}, \theta_{Lm}, u_{0m}, v_{0m}, w_{0m}, \theta_{0m})^T \quad (C33)$$

$K_{CSm}$  is the cylindrical-shell stiffness matrix,  $F_{ext m}^{CS}$  is the element external force vector,  $F_{int m}^{CS}$  is the element internal force vector, and the subscripts  $L$  and  $0$  denote locations at  $z = z_L$ , and  $z = z_0$ , respectively, and  $m$  denotes the FOURIER component number.

If stress calculation for cylindrical shell is desired, we can follow the similar procedure described in Remark vi of section B.

## Appendix D

### Procedure of Deriving TMB Finite Element

In Appendices A, B and C, it is shown that the governing equations for FOURIER components for shaft, end-disk plate with non-uniform thickness, and cylindrical shell of a pulley can be reduced to a set of ODEs of first order respectively, and these ODEs can be finally unified as the following form

$$\frac{d\psi_m}{ds} = H_m(s)\psi_m + L_m \quad (m = 0, \pm 1, \pm 2, \dots) \quad (D1)$$

where the subscript  $m$  denotes the ordinary number of FOURIER components,  $H_m$  is a  $2n \times 2n$  matrix,  $L_m$  is a  $2n \times 1$  vector containing external loads,  $\Psi_m$  is the state variable vector defined as

$$\psi_m = (U_m^T, F_m^T)^T \quad (D2)$$

$U_m$  is an  $n \times 1$  vector containing generalized displacements,  $F_m$  an  $n \times 1$  vector containing corresponding generalized internal forces, and  $s$  is an axial or radial coordinate of the pulley, which is assumed within the range of  $s_0 \leq s \leq s_L$ , where  $s_0$  and  $s_L$  are corresponding to two ends of a pulley component section (i.e. element).

Because Eq. (D1) is linear, the general solution is obtainable. By using the theory of ODE [8], the general solution to Eq. (D1) can be written as

$$\psi_m(s) = T_m(s)\psi_m(s_0) + T_m(s) \int_{s_0}^s T_m(x)^{-1} L_m(x) dx \quad (D3)$$

where  $T_m(s)$  is a  $2n \times 2n$  matrix called transfer matrix satisfying

$$\frac{dT_m}{ds} = H_m T_m \quad \text{and} \quad T_m(s_0) = I \quad (D4)$$

where  $I$  is the identity matrix. For any set of linear ordinary differential equations, which can be expressed in the form of Eq. (D1), there exists a unique  $2n \times 2n$  transfer matrix  $T_m(s)$  satisfying Eq. (D4). If Eq. (D1) is a set of constant ODEs (i.e.,  $H_m$  is independent of  $s$ ) or it can be transformed into a set of constant ODEs, a closed-form transfer matrix  $T_m(s)$  is obtainable. The general procedure of deriving  $T_m(s)$  is discussed in many textbooks, such as the one by BOYCE and DiPRIMA [8]. In what follows in this section, it is shown that a special finite element (i.e., TMB element) can be developed from Eq. (D3).

Let us consider a section of pulley, which is located in  $s_0 \leq s \leq s_L$ , and let

$$T_m(s_L) = \begin{bmatrix} T_{UU} & T_{UF} \\ T_{FU} & T_{FF} \end{bmatrix} \quad (D5)$$

$$\psi_m(s_L) = \begin{bmatrix} U_L \\ F_{int L} \end{bmatrix} \quad (D6)$$

$$\psi_m(s_0) = \begin{bmatrix} U_0 \\ -F_{int 0} \end{bmatrix} \quad (D7)$$

$$P_m = T_m(s_L) \int_{s_0}^{s_L} T_m(x)^{-1} B(x) dx \quad (D8)$$

where

$$U_L = U_m(s_L) \quad (D9)$$

$$U_0 = U_m(s_0) \quad (D10)$$

$$F_{int L} = F_m(s_L) \quad (D11)$$

$$F_{int 0} = -F_m(s_0) \quad (D12)$$

Then Eq. (D3) can be rewritten as

$$\begin{bmatrix} U_L \\ F_{int L} \end{bmatrix} = \begin{bmatrix} T_{UU} & -T_{UF} \\ T_{FU} & -T_{FF} \end{bmatrix} \begin{bmatrix} U_0 \\ F_{int 0} \end{bmatrix} + P_m \quad (D13)$$

Reorganizing Eq. (D13), we have

$$\begin{bmatrix} I & -T_{UU} \\ 0 & -T_{FU} \end{bmatrix} \begin{bmatrix} U_L \\ U_0 \end{bmatrix} = \begin{bmatrix} 0 & -T_{UF} \\ -I & -T_{FF} \end{bmatrix} \begin{bmatrix} F_{int L} \\ F_{int 0} \end{bmatrix} + P_m \quad (D14)$$

from which we can obtain

$$K_m D_m = F_{int m} + F_{ext m} \quad (D15)$$

where

$$K_m = \begin{bmatrix} 0 & -T_{UF} \\ -I & -T_{FF} \end{bmatrix}^{-1} \begin{bmatrix} I & -T_{UU} \\ 0 & -T_{FU} \end{bmatrix} \quad (D16)$$

$$D_m = (U_L^T, U_0^T)^T \quad (D17)$$

$$F_{int m} = \begin{bmatrix} F_{int L} \\ F_{int 0} \end{bmatrix} \quad (D18)$$

$$F_{ext m} = \begin{bmatrix} 0 & -T_{UF} \\ -I & -T_{FF} \end{bmatrix}^{-1} P_m \quad (D19)$$

It is seen that Eq. (D15) is formulated in a finite-element form, where  $K_m$  is element stiffness matrix,  $D_m$  is the element displacement vector,  $F_{int m}$  is the element internal force vector, and  $F_{ext m}$  is the element external force vector. The detailed procedures of developing TMB elements for shaft, end-disk and cylindrical shell are given in Appendices A, B and C, respectively.

#### Remarks:

- It is noted that in developing TMB finite elements the trial function for representing element displacement field is not required. This is the feature that distinguishes the MTM method from the conventional finite element method.
- In general, for any type of structures, whose governing differential equations can be reduced to the form of Eq. (D1), which can be further transformed into a set of constant ODEs, the corresponding transfer matrix  $T_m(s)$  of Eq. (D3) can be derived following some standard procedure described in [8]. In most cases, the procedure of deriving  $T_m(s)$  can be fulfilled by using a computer program, and  $P_m$  defined in Eq. (D8) can be evaluated analytically or numerically; and therefore, a computer program can be made, where the input is the matrix  $H_m$  and the external loads, and the output is the TMB element stiffness matrix and element external force vector. In this program, there is no discretization error in computing TMB element stiffness matrix. As a FORTRAN subroutine, such a computer program has been developed in PSTRESS 3.0.

For more information on Precision Pulley  
circle Reader Service Card No. 14